sciendo

Ekológia (Bratislava) - Journal of the Institute of Landscape Ecology, Slovak Academy of Sciences Vol. 41, No. 2, p. 113–125, 2022

DOI:10.2478/eko-2022-0012

INFLUENCE OF PLANTS ON THE SPATIAL VARIABILITY OF SOIL PENETRATION RESISTANCE

OLGA KUNAKH ✉[1], YULIA ZHUKOVA[2], VOLODYMYR YAKOVENKO[3], OLGA DANIUK[4]

[1]Department of Zoology and Ecology, Faculty of Biology and Ecology, Oles Honchar Dnipro National University, Gagarin Ave. 72, 49010 Dnipro, Ukraine; e-mail: kunah_olga@ukr.net

[2]Department of Zoology and Ecology, Faculty of Biology and Ecology, Oles Honchar Dnipro National University, Gagarin Ave. 72, 49010 Dnipro, Ukraine; e-mail: karomeluka@gmail.com

[3]Department of Geobotany, Pedology, and Ecology, Faculty of Biology and Ecology, Oles Honchar Dnipro National University, Gagarin Ave. 72, 49010 Dnipro, Ukraine; e-mail: yakovenko_v@i.ua

[4]Department of Ecology, General Biology, and Environmental Management, Bogdan Khmelnitsky Melitopol State Pedagogical University, Hetmanska st., 20, Melitopol, 72318, Ukraine; O1986dan@gmail.com

✉ Corresponding author

Received: 17 November 2021 / **Accepted:** 4 May 2022

Abstract

Kunakh O., Zhukova Y., Yakovenko V., Daniuk O.: Influence of plants on the spatial variability of soil penetration resistance. Ekológia (Bratislava), Vol. 41, No. 2, p. 113–125, 2022.

Soil penetration resistance is an informative indicator to monitor soil compaction, which affects a range of ecological processes in floodplain ecosystems. The aim of the investigation was to reveal the influence of vegetation cover on the spatial variability of penetration resistance of floodplain soils. The study was carried out in the elm oak forest in the floodplain of the Dnipro River (Dniprovsko-Orilsky Nature Reserve, Ukraine). The study of the soil profile morphology was performed in accordance with the guidelines of the field description of soils FAO. The soil penetration resistance was measured in the field using the Eijkelkamp manual penetrometer to a depth of 100 cm at 5-cm intervals within the polygon consisted of 105 sampling points. Vegetation descriptions were made in a 3×3-meter surrounding from each sampling point. The soil penetration resistance was found to regularly increase with increasing depth. The changes in resistance values were insignificant until 25–30 cm depth. After that, there was a sharp increase in penetration resistance up to the depth of 70–75 cm, after which the indicators plateaued. In the three-dimensional aspect, the spatial variation of soil penetration resistance can be fractionated into broad-scale, medium-scale, and fine-scale components. Tree vegetation induces a broad-scale component of soil penetration resistance variations, which embraces the whole soil profile. The herbaceous vegetation induces a medium-scale component, which embraces the upper and middle parts of the soil profile. The fine-scale component is influenced by pedogenic factors.

Key words: soil compaction, floodplain, distance-based Moran's eigenvector maps, community ordination, phytoindication.

Introduction

Penetration resistance is a physical property of soil that depends on soil texture and bulk density (Mohanty et al., 2004; Imhoff et al., 2016), moisture content (Vaz et al., 2001; Junior et al., 2014), porosity and permeability (Holthusen et al., 2018), particle size distribution (Dexter et al., 2007), structure, mineral and organic matter content of soil (Medvedev, 2009; Yao et al., 2015), pH, cation-exchange capacity, clay particle thickness, and presence of iron oxides and free aluminum hydroxide, which determine the nature of the resulting cohesive forces between soil constituent (Assouline et al., 1997). The soil penetration resistance is an informative indicator for monitoring soil compaction (Benevenute et al., 2020). The soil compaction increases the resistance of the soil to plant root growth (Unger, Kaspar, 1994; Correa et al., 2019) impedes the movement of soil animals (Lamandé et al., 2003; Plum, 2005) reduces porosity, which slows water transfer and air diffusion; and decreases the rate of mineralization of nutrients (De Neve, Hofman, 2000). The soil compaction modifies the soil moisture regime and can inhibit root growth if certain boundary levels are exceeded, resulting in the plant not being able to obtain water or nutrients at depth (Sinnett et al., 2008). Poor root development makes mature trees more susceptible to windthrow (Bécel et al., 2012). The compactness of anthropogenic soils is a consequence of technological procedures (Zhukov, Gadorozhnaya, 2016; Zadorozhnaya et al., 2018). Therefore, the study of soil penetration resistance is often performed to assess the effect on crop yields (Schjønning et al., 2016; Colombi et al., 2018) or tree growth dynamics in forest plantations (Krzic et al., 1999; Labelle et al., 2019). The soil penetration resistance was shown to be an important attribute of the ecological niche of mollusks under land reclamation (Kunakh et al., 2018; Yorkina et al., 2018). The soil penetration resistance along with other morphological and physical properties is used to diagnose

© The Author(s) 2022. This is an open access article licensed under the Creative Commons Attribution-NonCommercial-NoDerivs License (http://creativecommons.org/licenses/by-nc-nd/3.0/).

urban soils (Prokof'eva et al., 2021) and is a reliable indicator of recreational load (Yorkina et al., 2020; Budakova et al., 2021). The natural soils receive much less attention in this respect (Yakovenko, Zhukov, 2021).

The regulatory role of soil penetration resistance in natural soils is also important, even though there are no effects that are caused by excessive anthropogenic influences. The study of anthropogenic soils attracts attention when the soil impedance increases as the most probable cause of decreased productivity of plant communities. In the natural ecosystems in the floodplain, low soil impedance can be a marker of soil dynamism and be the cause of disorganization of the community structure of soil macrofauna (Zhukov et al., 2017, 2018). Reduced soil compaction was shown to support the development of non-native plant species populations. Invasive species are sensitive to the amount of available nutrients in the soil, and reducing soil compaction allows root systems to penetrate deeper and makes more nutrients available (Kyle et al., 2007). There is an optimum level of soil compaction for root growth, but because natural soils are often very heterogeneous, the roots of plants growing in such environments are likely to experience a range of bulk soil densities and may well respond to such local changes (Tracy et al., 2011).

Plants affect the compactness of the soil. Tree stands in a riparian mixed forest are a significant factor structuring both the herbaceous community and the spatial variation of soil physical properties (Yakovenko, 2017; Zhukova et al., 2020). The roots transmit the weight of the trees into the soil, compacting it (Kozlowski, 1999). As roots expand, they penetrate through the soil and modify the physical, chemical, and biological properties in the surrounding area, the rhizosphere (Fageria, Stone, 2006). These changes can persist after root degradation, forming a branched system of associated biopores (Lucas et al., 2019). Natural disturbances such as geological events, glacial activity, or soil sliding can change the degree of the soil compaction on a large scale (Nawaz et al., 2013; Wang et al., 2020). Alternating wetting and drying can compact the soil as a result of swelling and shrinkage processes (Boivin et al., 2006). Sandy topsoil saturation during flooding can cause significant settling of soil particles to increase compaction. Slumping consequently follows the weakening of soil aggregates due to wetting and partial disintegration at contact points, allowing the aggregates to pack more densely (Xu et al., 2017; Nsabimana et al., 2020). On a smaller scale, the soil can be compacted or loosened by trampling, burrowing, and digging by animals (Roesch et al., 2019).

The technique of measurement of this attribute allows to collect in a relatively short period of time significant amounts of data on the spatial variability both in the horizontal and in the vertical directions. Thus, the soil penetration resistance is a good indicator of the variability of soil properties and can be applied to assess the spatial organization of the soil body. The usage of geostatistical and multivariate analysis allowed to evaluate the soil penetration resistance both vertically and horizontally. The multivariate analysis provided an opportunity to establish homogeneous zones with similarity both vertically and horizontally (Medina et al., 2012). For both anthropogenic soils and natural ones, the study of the influence of various causes on the variability of the soil penetration resistance is of interest.

The aim of this article is to identify the influence of vegetation cover on the spatial variability of soil penetration resistance of floodplain soils.

Material and methods

Study area

The study was carried out in the elm oak forest in the floodplain of the Dnipro River (Dniprovsko-Orilsky Nature Reserve, Ukraine) (48.50˚N 34.77˚E). Soil properties were measured at 105 points, which were located on a regular grid (Fig. 1). The points are located in the center of 3×3 m squares, within which the relevés was made. The squares are contiguous with each other, constituting a polygon. On the opposite corners of the polygon were placed locations where vertical soil transects were made.

Description of soil morphology

The study of the soil profile morphology was performed in accordance with the guidelines of the field description of soils FAO (Jahn et al., 2006). Genetic type of soil profile was determined according to Rozanov (Rozanov, 2004). The classification of soils was performed according to IUSS Working Group WRB (WRB, 2014).

Plant community description

The vegetation description was performed at polygon consisted of 105 sampling points (relevés). The points were located along 7 transects with 15 sampling points each. The distance between points in the transect as well as the distance between transects was 3 m. The adjacent sampling points were in close proximity to each other. Vascular plant species lists were recorded for each 3×3 m sampling point, along with a visual assessment of species coverage using a Braun-Blanquet scale (Westhoff, Van Der Maarel, 1978). The projective cover of plant species was measured at soil level, understory (up to 2 m in height), and canopy (above 2 m in height). Seedlings and seedlings of tree species were subsequently excluded from the analysis. Plant taxonomic names follow the Euro+Med Plantbase resource (http://ww2.bgbm.org/EuroPlusMed). A phytoindication of environmental factors was performed based on the Didukh (Mohanty, Patra, 2012).

Soil properties measurement

The soil penetration resistance was measured in the field using the *Eijkelkamp* manual penetrometer, to a depth of 100 cm at 5-cm intervals (Zhukov, Gadorozhnaya, 2016; Zhukov et al., 2019). The average error of the measurement results of the device is ± 8%. Measurements were made with a cone with a cross section of 1 cm^2. At each measurement point, the soil penetration resistance was performed in only one replication.

Statistical analysis

The phytoindication estimates of environmental factors obtained on the basis of species composition and grass projective cover were used as predictors of the environment, as well as data on the crown cover of trees. The data on crown density and projective cover of herbaceous plants (proportion in the range from 0 to 1) were transformed: $\text{asin}((c_i)^{0.5})$, where c_i is the projective cover of

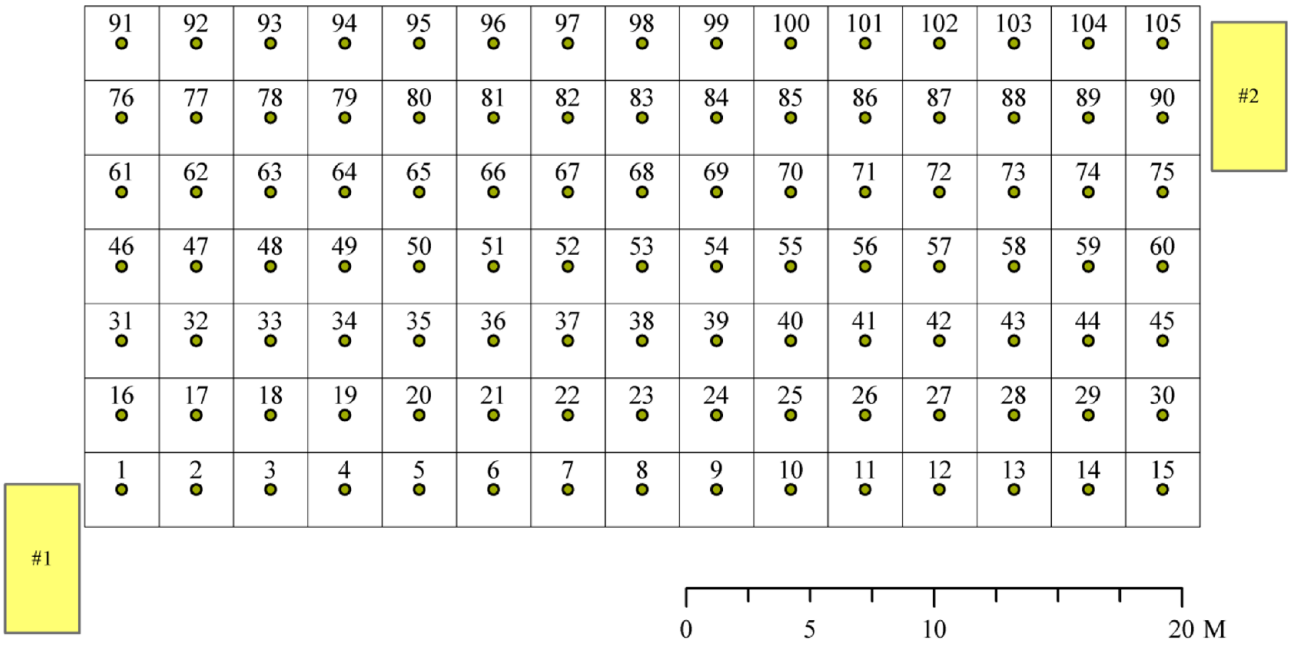


Fig. 1. Scheme of the location of sample sites and soil sections. The points 1, ..., 105 indicate the locations where soil properties were measured. The squares denote vegetation description locations. Rectangles denote locations of soil sections #1 and #2.

the *i*-th species. Species that occurred in the relevés at least 10 times were selected for the ordination procedure. There were 18 such species. The ordination of the plant community was performed using the method of nonmetric scaling (Kruskal, 1964) using the Bray-Curtis distance (Bray, Curtis, 1957; Warton et al., 2012). According to the criterion of decreasing stress, the ordinal solution with four dimensions was found to be optimal (Hout et al., 2013). The environmental factors were fitted to the ordinal dimensions using the *envfit* function from the *vegan* package (Oksanen et al., 2019).

The soil penetration resistance data for each soil layer were rescaled by standardization (or *Z*-score normalized), after which their mean value was set to zero, and the value itself was presented in units of standard deviation:

$$x_{stand} = \frac{x_{obs} - mean(x)}{standard\ deviation(x)}$$

where is observed value and is standardized value.

A matrix consisting of standardized soil penetration resistance values was subjected to a Redundancy Analysis (RDA) (Gilbert, Bennett, 2010; Dray et al., 2012). Based on the local coordinates of the sampling points, a distance matrix between points was generated. The distance-based Moran's eigenvector maps (Borcard, Legendre, 2002; Legendre, Legendre, 2012) were computed from the distance matrix using the function *dbmem* from the package *adespatial* (Dray et al., 2018). The 48 dbMEM eigenfunctions were extracted. Each of the dbMEM eigenfunctions models a spatial pattern with a frequency that increases in proportion to the order number of the function. The dbMEM eigenfunctions were used as predictors in the Redundancy Analysis procedure of standardized soil penetration resistance data. The explanatory power of the predictors in the Redundancy Analysis was estimated using the function *RsquareAdj2.rda* (Zelený, 2016). A scalogram was constructed by estimating R^2 for each spatial predictor separately. The vegetation ordination dimensions were also considered as conditional predictors. Three-dimensional mapping of soil penetration resistance isolines was performed in the software program Voxler® 4.2.584.

Results

Soil morphology

The vertical cross section of soil #1: The description was performed on October 5, 2018, in the Dniprovsko-Orilsky Nature Reserve. The soil section was placed on a flattened area of the floodplain (Fig. 2A). The character of the soil surface was undulating. The vegetation was represented by elm oak. The projective cover of the grass stand was 40–60%. The forest litter was 2–3 cm thick and consisted of tree leaves and herbaceous plant residues. The projective cover of the forest litter was 30–40%. The soil-forming bedrock was represented by alluvial sandy sediments. The groundwater level was 140 cm. There were occasional traces of soil invertebrate activity, which had no significant effect on horizon mixing. There was no boiling from HCl in the soil profile. The genetic type of the profile was identified as hydrogenous differentiated and was polycyclic and stratified in structure. The classification position according to WRB was Fluvic Gleysol (Arenic, Ochric).

The vertical cross section of soil # 2: The description was performed on October 5, 2018, in the Dniprovsko-Orilsky Nature Reserve. The soil section was placed in a local lowering of the floodplain (Fig. 2B). The soil surface was undulating and flattened. The vegetation was represented by elm oak. The projective

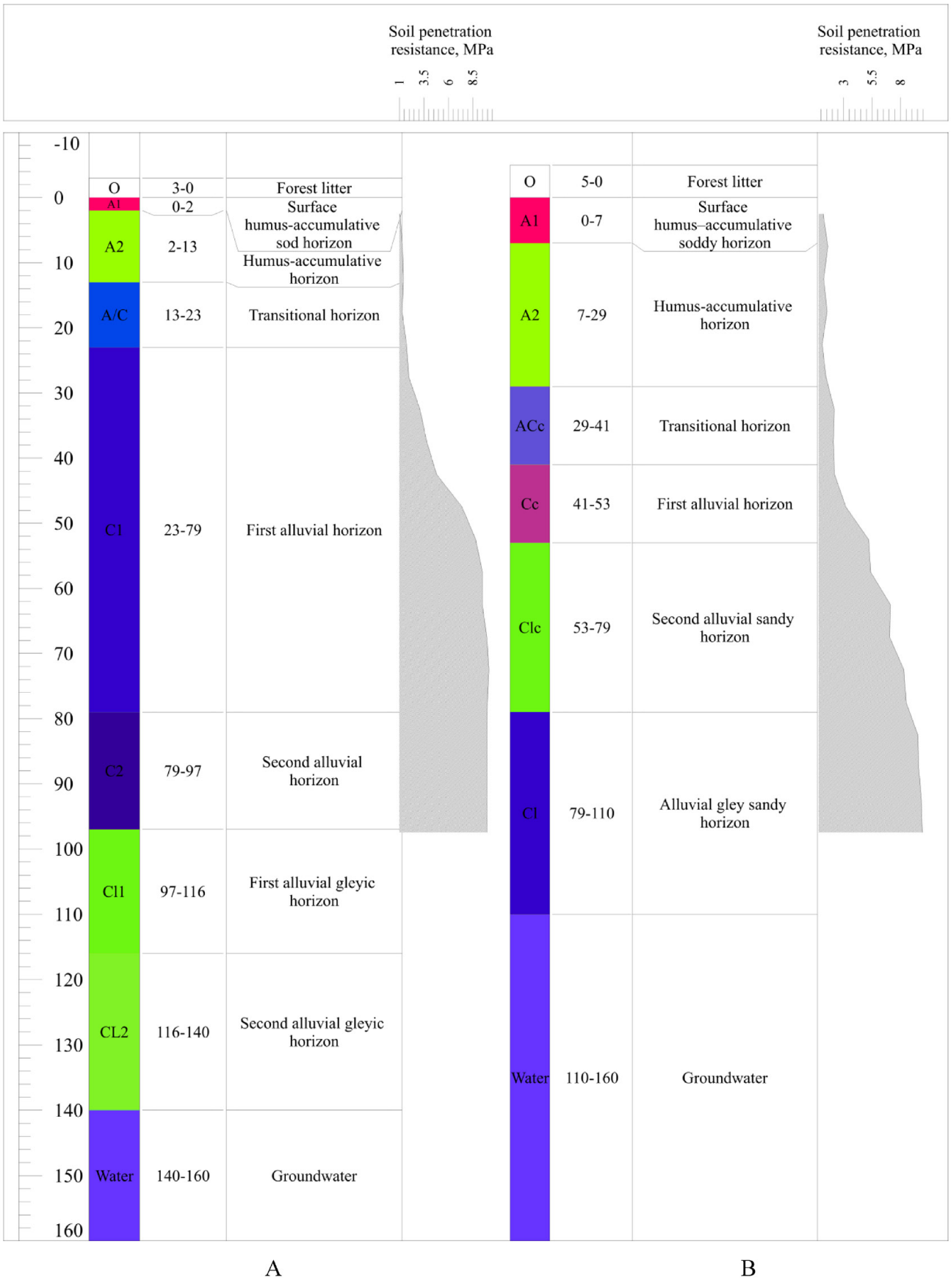


Fig. 2. Soil profile in section 1 (A) and section 2 (B).

A: O (3–0 cm) is the forest litter from leaves of trees and herbaceous plants of various degrees of destruction. A1 (0–2 cm) is the surface humus-accumulative, sod horizon. Light gray, dry, sandy loam. Unstructured, loose, abundantly interlaced by root systems of herbaceous plants. Easily separated from the next horizon. The transition to the next horizon is sharp in color, structure, density, and saturation by roots. A2 (2–13 cm) is the humus-accumulative horizon. Brown-gray with humus spots, fresh, sandy loam. Root saturated. The structure is dusty-grained, and the aggregates are not persistent, easily dispersed when pressed with fingers. Compaction is dense. The transition to the next horizon is gradual in color. A/C (13–23 cm) is the transitional horizon. The color is heterogeneous. On the background of the main mass of brown color, spots of light yellow color of different sizes with diffuse contours are observed. The texture is light loamy. Wet. The structure is dusty-grained, and the aggregates are easily broken when pressed. The compactness is dense. Roots of shrubs and trees are found. The existing root holes are colored with dark humus material of loose compactness. The transition to the next horizon is sharp undulating in color, granulometric composition, structure, and density. C1 (23–79 cm) is the first alluvial horizon. Light yellow in color with rusty spots that increase with depth. Sandy, unstructured, fresh. Occasionally, there are vertically oriented bands of material colored with organic matter. The transition to the next horizon is not clear 2–3 cm wide in color. C2 (79–97 cm) is the second alluvial horizon. Light gray, stratified. The layers of the humus material are 0.5–1 cm thick with an interval of 1.5–2 cm. The darker colored layers 0.5–1 cm thick alternate with light gray material 1.5–2 cm thick. Sandy, dense compact, moist. Tree roots occur. The transition to the next horizon in color and moisture is smooth, and the transition zone is 1.5 cm wide. Cl1 (97–116 cm) is the first alluvial gleyic horizon. Rusty gray with rusty spots and horizontal bands of the humus material. Sandy, loose compactness. The transition to the next horizon is abrupt in color and moisture. Cl2 (116–140 cm) is the second alluvial gleyic horizon. Loose wet sand. Brownish-gray and bluish-gray color corresponds to reducing conditions and gleyic properties. From a depth of 140 cm, there is groundwater.

B: O (5–0 cm) is the stratified forest litter composed of tree leaves and residues of herbaceous plants. Dry, easily scattered. A1 (0–7 cm) is the surface humus-accumulative, soddy horizon. Color brown to dark gray. Light loam. Loosely compact, abundantly interbedded with herbaceous root systems and decaying leaves. Finely coarse-grained, and the aggregates break up easily when pressed. The horizon material is easily separated from the next horizon. The transition to the next horizon is sharp in color, structure, and rootiness. A2 (7–29 cm) is the humus-accumulative horizon. Brown-gray with patches of more humus-accumulative material. Wet. Light loam. The structure was silty-grained, and the aggregates are not persistent and easily crumbled when pressed. The compactness was loose. There were roots of shrubs. The transition to the next horizon was sharp undulating in color. ACc (29–41 cm) is the transitional horizon. Gray with dark gray or rusty spots. Wet. Light loam. Unstructured, loose compactness. There were individual roots of bushes and trees. The transition to the next horizon was gradual in color, not clear. Cc (41–53 cm) is the first alluvial horizon. Light gray with irregularly shaped rusty spots that extend mostly horizontally. Wet. Sandy, unstructured, loosely compacted. There were roots of woody species. The transition to the next horizon was not distinct 2–3 cm wide in color. Clc (53–79 cm) is the second alluvial sandy horizon. Wet. Mottled in rusty-gray, grayish-blue and brownish colors. The horizon presented layers of humusy material 0.5–1 cm thick with an interval of 1.5–2 cm of background color material. The darker colored layers 0.5–1 cm thick alternated with light gray material 1.5–2 cm thick. Loose, unstructured sand. Roots of tree species occur. Transition to the next horizon by color and moisture. Cl (79–110 cm) is the alluvial gley sandy horizon. The color of the horizon was grayish-blue, rusty-gray, and dark gray, which is characteristic of reducing conditions. Loose compactness with horizontal dark gray gley patches and rusty layers. From a depth of 110 cm – groundwater.

cover of the grass layer was 10–20 cm. The forest litter was 5–6 cm thick with a projective cover of 30–40 cm. The soil-forming rock was alluvial sand. The groundwater level was at a depth of 110 cm. There was occasional evidence of soil invertebrate activity, which made a restricted pedoturbation impact. Soil boiling from HCl was absent. The genetic type of the profile was identified as hydrogenous differentiated. The structure type was polycyclic and layered. The classification position according to WRB was Fluvic Mollic Gleysol (Loamic, Humic).

Plant community ordination

The 52 plant species were identified in the vegetation cover of which 4 species (7.7% of the number of species) were phanerophytes, 9 species (17.3%) were nanophanerophytes, 25 species (48.1%) were hemi-cryptophytes, 9 species (17.3%) were therophytes, and 5 species (9.6%) were geophytes (Table 1). A nonmetric multivariate scaling provided to extract four dimensions. The NMDS1 dimension explained the opposite dynamics of autochthonous tree species on one hand and ruderal adventive species on the other. This dimension correlated strongly with the indicators of thermal regime, trophicity, and nitrogen nutrition. The NMDS2 dimension explained the opposite dynamics of *Ulmus laevis* on one side and *Pyrus communis* on the other. This dimension correlated strongly with the acidity, trophicity, and aeration regimes. The NMDS3 dimension correlated strongly with the soil carbonate content, soil aeration, and cryogenic regime. The NMDS3 dimension was strongly correlated with the light regime, moisture, and moisture variability.

Soil penetration resistance variation

The soil penetration resistance regularly increased with increasing depth (Table 2). The changes in resistance values were insignificant until 25–30 cm depth. After that, there was a sharp increase in penetration resistance up to the depth of 70–75 cm, after which the indicators plateaued. In the upper soil layer up to the depth of 55–60 cm, the coefficient of variation of soil penetration resistance was at the level of 16–28%, and with increasing depth, this index monotonically decreased. The skewness of distribution showed a tendency to decrease with depth. The skewness was greatest at a depth of 15–20 cm, where the distribution is most asymmetric with a shift to the left. The skewness was lowest at a depth of 85–90 cm, where the distribution showed the greatest shift to the right. The kurtosis was lowest at a depth of 65–70 cm, where the distribution was obviously bimodal. The kurtosis was greatest at a depth of 95–100 cm, where the distribution non-randomly tended to be modal.

Table 1. Species diversity of the plant community and the correlation of plant projective cover with dimensions obtained by nonmetric multidimensional scaling.

Life form*	Species	Crown enclosure or projective cover, %±st. error**	Ordination dimension			
			NMDS1	NMDS2	NMDS3	NMDS4
Ph	*Acer negundo* L.	0.45±0.09	–	–	–	–
	Pyrus communis L.	1.68±0.46	–	–	–	–
	Quercus robur L.	25.70±1.31	–	–	–	–
	Ulmus laevis Pall.	13.62±0.66	–	–	–	–
nPh	*Amorpha fruticosa* L.	4.28±0.42	–	–	–	–
	Caragana frutex (L.) C. Koch	+	–	–	–	–
	Crataegus fallacina Klokov	0.19±0.07	–	–	–	–
	Euonymus europaeus L.	0.08±0.04	–	–	–	–
	Euonymus verrucosus Scop.	+	–	–	–	–
	Frangula alnus Mill.	0.02±0.01	–	–	–	–
	Rhamnus cathartica L.	0.34±0.16	–	–	–	–
	Rubus caesius L.	2.56±0.33	0.54	0.31	–0.15	0.26
	Sambucus nigra L.	0.36±0.12	–0.88	0.32	0.09	–0.05
HKr	*Alliaria petiolata* (M.Bieb.) Cavara et Grande	3.36±0.34	–0.38	–0.08	–0.27	0.10
	Anthriscus sylvestris (L.) Hoffm.	0.24±0.06	–0.25	0.69	0.57	0.36
	Arctium lappa L.	0.21±0.08	–	–	–	–
	Asparagus officinalis L.	0.08±0.05	–	–	–	–
	Brachypodium sylvaticum (Huds.) P. Beauv.	0.03±0.03	–	–	–	–
	Calystegia sepium (L.) R.Br.	0.14±0.07	–	–	–	–
	Carex acuta L.	+	–	–	–	–
	Carex vulpina L.	0.10±0.05	–	–	–	–
	Chelidonium majus L.	0.10±0.04	–	–	–	–
	Cynoglossum officinale L.	0.06±0.03	–	–	–	–
	Erysimum aureum M.Bieb.	0.03±0.03	–	–	–	–
	Festuca drymeja Mert. & W.D.J. Koch	0.15±0.06	–	–	–	–
	Geranium robertianum L.	0.06±0.04	–	–	–	–
	Geum urbanum L.	2.21±0.18	0.28	–0.11	0.18	–0.29
	Glechoma hederacea L.	5.91±0.46	0.01	–0.28	0.29	0.05
	Leonurus quinquelobatus Gilib.	0.19±0.06	–0.30	–0.37	0.00	0.93
	Lithospermum officinale L.	+	–	–	–	–
	Lycopus europaeus L.	0.02±0.01	–	–	–	–
	Lysimachia nummularia L.	2.43±0.44	0.13	0.69	0.44	0.30
	Poa nemoralis L.	0.37±0.11	–0.41	0.17	–0.36	–0.13
	Silene baccifera (L.) Roth	0.11±0.05	–	–	–	–
	Silene latifolia Poir.	+	–	–	–	–
	Symphytum officinale L.	0.14±0.05	–0.63	–0.16	0.93	–0.10
	Urtica dioica L.	3.36±0.34	–0.50	0.27	0.23	–0.13
	Veronica chamaedrys L.	+	–	–	–	–
T	*Anthriscus cerefolium* (L.) Hoffm.	1.03±0.23	0.10	0.39	–0.46	0.10
	Atriplex micrantha C. A. May	0.27±0.14	–	–	–	–
	Galium aparine L.	2.25±0.18	0.03	0.04	–0.09	–0.34
	Lactuca serriola L.	+	–	–	–	–
	Lapsana communis L.	0.04±0.03	–	–	–	–
	Polygonum aviculare L.	0.32±0.08	0.56	–0.10	–0.09	–0.39
	Stellaria media (L.) Vill	0.16±0.07	–	–	–	–
	Vicia tetrasperma (L.) Schreb.	0.84±0.17	0.23	–0.56	0.02	0.47
	Viola arvensis Murr.	0.70±0.14	0.16	–0.65	–0.35	0.51
G	*Alopecurus pratensis* subsp. *arundinaceus* (Poir.) Husn.	+	–	–	–	–
	Aristolochia clematitis L.	0.16±0.06	0.98	0.55	0.16	0.54
	Calamagrostis epigeios (L.) Roth	0.30±0.11	–	–	–	–
	Convallaria majalis L.	6.59±0.57	0.07	–0.08	–0.31	–0.11
	Elymus repens (L.) Gould	0.29±0.14	–	–	–	–

Notes: * – Raunkiær plant life form (Raunkiaer, 1937): Ph – phanerophytes, nPh – nanophanerophytes, HKr – hemi-cryptophytes, T – therophytes, G – geophytes, ** – in the table "+" indicates a single appearance of plants.

Table 2. Descriptive statistics of the variation of soil penetration resistance (N = 105).

Layer, cm	Mean±st. error, MPa	Coefficient of variation, %	Skewness±st. error	Kurtosis±st. error
0–5	1.29±0.023	18.67	0.03±0.24	–0.31±0.47
5–10	1.50±0.035	23.86	–0.01±0.24	–0.32±0.47
10–15	1.46±0.033	22.89	0.14±0.24	–0.58±0.47
15–20	1.45±0.022	15.60	0.57±0.24	0.14±0.47
20–25	1.51±0.026	17.50	0.16±0.24	–0.55±0.47
25–30	1.85±0.044	24.23	0.17±0.24	–0.04±0.47
30–35	2.44±0.051	21.47	0.11±0.24	–0.09±0.47
35–40	3.07±0.082	27.56	0.08±0.24	–0.58±0.47
40–45	3.83±0.103	27.68	0.03±0.24	–0.43±0.47
45–50	5.02±0.111	22.69	0.42±0.24	0.01±0.47
50–55	6.18±0.133	22.13	0.07±0.24	0.04±0.47
55–60	7.36±0.134	18.71	–0.18±0.24	0.08±0.47
60–65	8.10±0.105	13.31	0.12±0.24	–0.70±0.47
65–70	8.70±0.098	11.49	–0.05±0.24	–1.11±0.47
70–75	9.05±0.088	9.91	–0.07±0.24	–0.73±0.47
75–80	9.40±0.060	6.49	–0.25±0.24	–0.42±0.47
80–85	9.64±0.030	3.16	–0.10±0.24	–0.28±0.47
85–90	9.88±0.023	2.44	–0.42±0.24	–0.18±0.47
90–95	9.94±0.013	1.29	–0.25±0.24	0.25±0.47
95–100	9.96±0.008	0.80	–0.07±0.24	0.37±0.47

Table 3. Fitting ecological parameters to dimensions derived after nonmetric multidimensional scaling of herbaceous vegetation.

Predictor*	Ordination dimension				R^2	*p*-level
	NMDS1	NMDS2	NMDS3	NMDS4		
Phytoindication scales						
Hd	–0.20	0.13	0.60	–0.76	0.04	0.43
fH	0.36	–0.52	0.43	0.65	0.17	<0.001
Rc	–0.06	0.85	0.53	–0.01	0.28	<0.001
Sl	–0.52	0.61	0.50	0.33	0.25	<0.001
Ca	–0.02	–0.35	–0.83	0.43	0.14	0.01
Nt	–0.84	0.54	0.01	–0.01	0.06	0.18
Ae	–0.38	0.58	0.67	–0.24	0.31	<0.001
Tm	–0.91	–0.38	–0.04	–0.18	0.08	0.08
Om	0.18	–0.61	–0.58	0.52	0.07	0.12
Kn	–0.29	–0.74	–0.35	0.49	0.05	0.23
Cr	0.20	–0.65	0.72	–0.16	0.14	0.01
Lc	–0.42	–0.18	0.43	0.78	0.10	0.04
Crown enclosure of tree species						
Acer negundo	0.24	0.08	0.75	–0.61	0.07	0.11
Pyrus communis	–0.59	–0.67	0.27	0.35	0.24	<0.001
Quercus robur	–0.64	–0.24	0.20	–0.70	0.26	<0.001
Ulmus laevis	–0.50	0.84	0.19	0.12	0.10	0.03
Amorpha fruticosa	0.74	0.43	0.37	–0.36	0.19	<0.001
Crataegus fallacina	0.38	0.58	0.54	0.47	0.04	0.40

Notes: * *Hd* – the soil water regime (mean indicator value 12.8±0.14 is optimal for mesophytes), *fH* – the variability of damping (mean indicator value 6.5±0.10 is optimal for hemi-hydrocontrastophobes – plants adapted to fresh forest-meadow habitats with moderately irregular wetting of soil layer fully drenched by precipitations), *Rc* – the soil acidity (mean indicator value 8.1±0.05 is optimal for sub-acidophiles – plants which grow on faintly acid (pH=5.5–6.5) forest soil, meadow marsh habitats), *Sl* – the total salt regime (mean indicator value 5.0±0.05 is optimal for mesotrophes dwelling on soils not reach on salt), *Ca* – the carbonate content in soil (mean indicator value 5.5±0.10 is optimal for hemi-carbonatophobes – plants avoiding carbonate substrates), *Nt* – the nitrogen content in soil (mean indicator value 6.9±0.11 is optimal for hemi-nitrophiles – plants which grow on soils moderately rich in mineral nitrogen), *Ae* – the soil aeration (mean indicator value 5.9±0.07 is optimal for hemi-aerophobes – plants which grow on the moderately aerated soils), *Tm* – the thermal climate (mean indicator value 10.2±0.08 is optimal for sub-mesotherms which indicates radiation balance to be equal to 2137 $MJ*m^{2}*year^{-1}$), *Om* – the ombroregime (mean indicator value 12.7±0.09 indicates a difference between annual precipitation quantity and evaporation to be equal to –44.1 mm), *Kn* – the continentality (mean indicator value 5.8±0.13 is optimal for sub-oceanic ecogroup), *Cr* – the cryo-climate (mean indicator value 9.8±0.06 is optimal for hemi-cryophytes which indicates the temperature of the coldest months to be equal to –1.4˚C), Lc – the light regime (mean indicator value 7.8±0.07 is optimal for sub-heliophytes – plants of light forests and shrubberies).

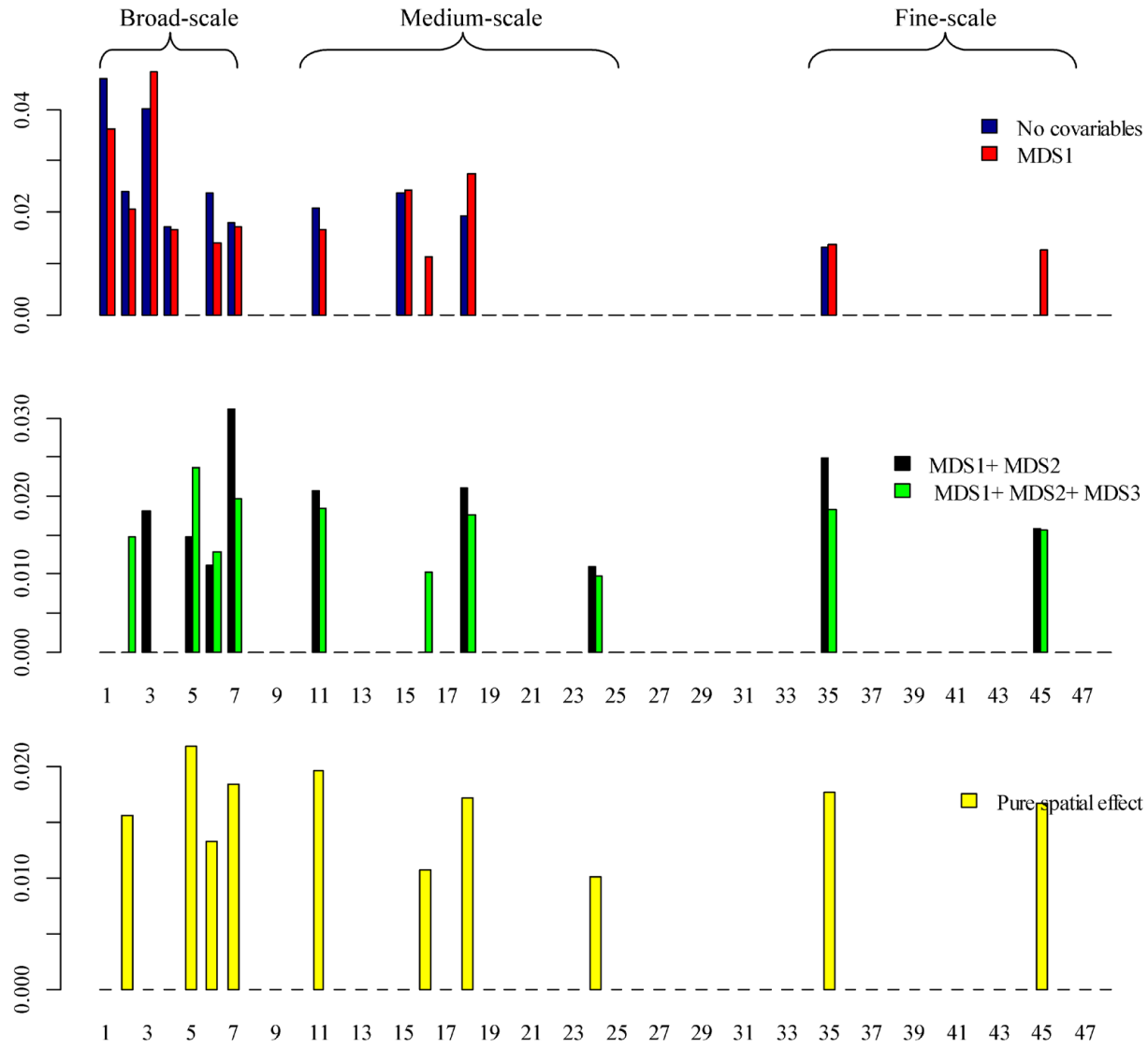


Fig. 3. Scalogram of spatial variables with different predictors as conditional covariates. The abscissa axis is the ordinal numbers of the dbMEM variables; the ordinate axis is the explained variation of the standardized value of soil penetration resistance by the respective dbMEM variable.

The dbMEM eigenfunctions were able to explain 46.7% of the variation in soil penetration resistance ($F = 2.90$, $p < 0.001$). The broad-scale spatial components (dbMEM eigenfunctions 1, 3, 4, 5, 6, 7) were able to explain 16.3% of the variation ($F = 4.38$, $p < 0.001$), the medium-scale components (dbMEM eigenfunctions 11, 18) were able to explain 4.05% of variation ($F = 3.19$, $p < 0.001$), and the fine-scale components (dbMEM eigenfunctions 32, 35, 43) are able to explain 1.26 % of variation ($F = 1.44$, $p < 0.001$). Accounting for the MDS1 dimension as a conditional variable resulted in a decrease in the explanatory power of the spatial variables ($R_{adj}^2 = 42.8\%$, $F = 2.61$, $p < 0.001$). The scalogram indicated that for many of the spatial variables, the explanatory power decreased, but for variables 3, 16, 35, and 45, the explanatory power increased (Fig. 3). Including MDS1 and MDS2 dimensions as a conditional variable significantly decreased the explanatory power of the spatial variables ($R_{adj}^2 = 33.8\%$, $F = 2.09$, $p < 0.001$). The vegetation features that were explained by the MDS2 dimension conditioned the spatial patterns that were described by the broad-scale dbMEM eigenfunctions 1–4 and the medium-scale dbMEM eigenfunction 15. Accounting for MDS1 and MDS2 as conditional variables increased the explanatory power of dbMEM eigenfunction 5, 18, 24, 34, and 45. Accounting for MDS1, MDS2, and MDS3 dimensions as a conditional variable also decreased the explanatory power of dbMEM eigenfunctions 3, 7, 11, 18, 24, and 35 ($R_{adj}^2 = 29.5\%$, $F = 1.87$, $p < 0.001$). In contrast, the explanatory power of dbMEM eigenfunctions 2, 5, and 16 increased. Accounting as conditional variables for all measurements that were derived from the vegetation ordination allowed for an estimate of the pure spatial component of the variation in the soil penetration tolerance. Accounting for MDS1, MDS2, MDS3, and MDS4 dimensions as a conditional variable explained 29.5% of the variation in the

soil penetration resistance (F = 1.85, p < 0.001). This indicates that the importance of the MDS4 dimension was insignificant in forming variability in the soil penetration resistance.

The analysis of the spatial variation of the soil penetration resistance (Fig. 4) and its fractions induced by different causes (Fig. 5), as well as the information on the correlation of this index with NMDS dimensions (Table 3), indicated that the spatial patterns of variation of the soil penetration resistance embraced all soil layers. The purely spatial pattern was characterized by the minimum structuring influence for the upper soil layers (0–20 cm) and the maximum structuring influence for the middle soil layer (25–35 cm). Each of the vegetative dimensions makes its own contribution to the mentioned differentiation. The influence of the MDS4 dimension on the soil penetration resistance is negligible. The role of the vegetation dimensions decreases with depth.

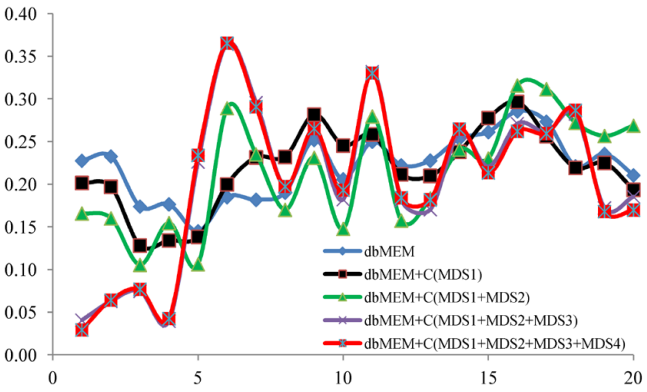


Fig. 4. Correlation of soil penetration resistance with axes obtained after RDA procedure with the spatial variables as predictors and ordinate dimensions as conditional variables: abscissa axis is the order of soil layers 0–5, 5–10, ..., 95–100 cm; ordinate axis is correlation coefficients with RDA axes; dbMEM is spetial eigenfunctions as predictors; and MDS1, ..., MDS4 are dimensions obtained in results of multidimensional vegetation scaling applied as conditional variables.

Discussion

Two types of soil were represented within the experimental polygon: Fluvic Gleysol (Arenic, Ochric) and Fluvic Mollic Gleysol (Loamic, Humic). The profile distribution of soil penetration resistance within the entire polygon has a common pattern. The compaction slightly increases with depth in the surface humus-accumulative sod horizon, humus-accumulative horizon, and transitional horizon. Within the alluvial horizons, there is a sharp increase in soil compaction, and in the deeper horizons, compaction changes insignificantly with depth. In addition to the general profile pattern of compactness variability, the relative changes in this parameter within one layer are important. The relatively lower compaction along the horizontal level may mark the zone of preferential water flow in the soil. The preferential flows significantly affect the water regime and ecological conditions of the soil (Zhang et al., 2018). Soil compaction can reduce the strength of the preferential flow due to the disruption of macropore continuity. An increase in inferential flow strength due to compaction was also shown (Mossadeghi-Björklund et al., 2016). Penetration resistance is a reliable indicator of soil compaction and preferential water flow in the soil profile (Mossadeghi-Björklund et al., 2019). The values of soil penetration resistance in a standardized form provide a detrended index, which indicates the differential ability of the soil to penetrate or migration of water. The standardized values represent, in units of root-mean-square deviation, the penetration resistance values at different soil layers. The indicators presented in the same units become comparable. The existing approaches to three-dimensional mapping of soil penetration resistance reproduce isolines of the same soil impedance (Castrignanò et al., 2004; Tekin et al., 2008). The standardized values of soil penetration resistance allowed to obtain three-dimensional "tomograms" of the soil body. Three-dimensional diagrams show the pattern of transition between two types of soils.

The concept of hierarchy of structural levels of soil organization describes the relationship between different structural elements of soil (Voronin, 1984; Yudina et al., 2018). The genetic conditions of soils give rise to a dual differentiation of pedological or soil horizons: by their vertical arrangement and by their spatial distribution. The first corresponds to the conventional notion of a soil profile, or solum, or sequence of soil horizons viewed in a vertical section. The second corresponds to the lateral arrangement of the different types of horizons within a landscape, which allows the definition of soil systems (Ditzler et al., 2002). Three-dimensional diagrams reveal that the soil body consists of three-dimensional morphological structures, the scale level of which exceeds the level of the morphological profile, but is lower than the pedon level. The transition between soil types is not abrupt, but it is the result of a change in the proportion between morphological elements of the same type. These morphological elements are pedogenic and biogenic in nature. The phytogenic component was considered in the study, but the zoogenic role in the formation of morphological structures cannot be excluded.

The morphological structures of the soil scale above the soil profile but below the pedon are very diverse and fuzzy. An adequate model for such soil morphological formations is a wave process of varying frequency. The morphological patterns of soil compaction can be fractionated into broad-scale, medium-scale, and fine-scale spatial components. The generation of frequency patterns of different scales is due to different causes. The broad-scale component is caused by trees, and the influence of this factor covers the entire soil profile studied. In a natural floodplain forest, distance from trees was shown to be a factor that determines the spatial pattern of variation in soil penetration resistance. In turn, soil resistance affects the species composition of the forest herbaceous layer (Zhukov et al., 2019). Tree species transfer wind energy through oscillatory movements of the trunk and roots into the soil (Netsvetov, Nikulina, 2010). At the same time, each tree species is characterized by specific spectral features of the oscillatory process it generates (Kovacic et al., 2018). Trees influence the variability of soil properties by regulating the availability of resources to plant species from other layers (Jones et al., 1994; Flinn, Marks, 2007). The regulation of the light regime is the most important mechanism of the influence of trees on the grass layer of the

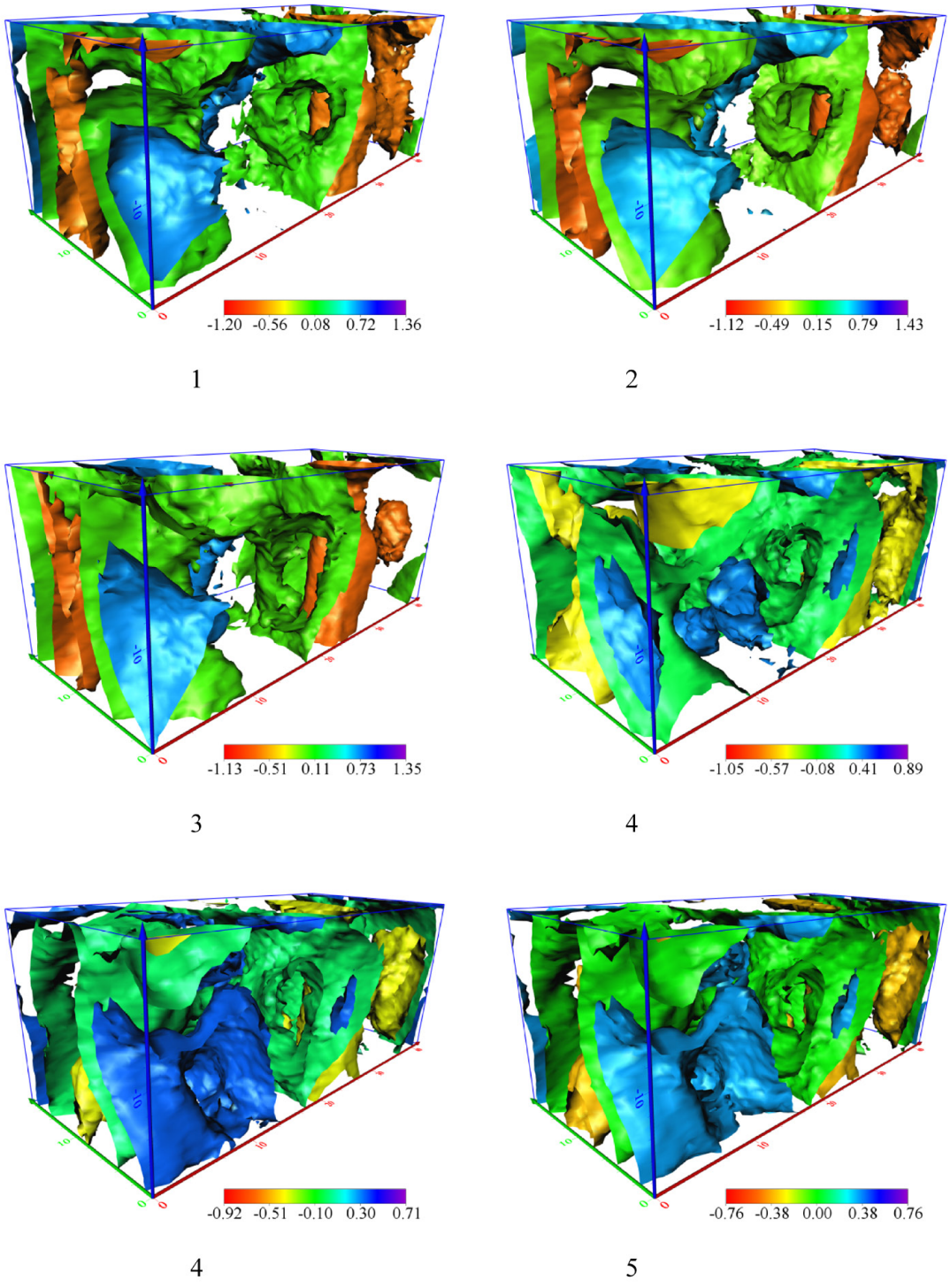


Fig. 5. Isolines of soil penetration resistance in 3D space. The soil penetration resistance is presented after standardization of the values within one layer: (1) the observed values are presented (warm color corresponds to isoline –0.7, green color corresponds to isoline 0, and cold color corresponds to isoline 0.7); (2) the values are presented which modeled by the spatial variables (warm color corresponds to isoline –0.7, green color corresponds to isoline 0, and cold color corresponds to isoline 0.7); (3) the values are presented which modeled by the spatial variables with plant axis MDS1 as covariate (warm color corresponds to –0.7 isoline, green color corresponds to 0 isoline, and cold color corresponds to 0.7 isoline); (4) the values are presented which modeled by the spatial variables with plant axes MDS1 and MDS2 as covariate (warm color corresponds to –0.4, green color corresponds to isoline 0, and cold color corresponds to isoline 0.4); (5) the values are presented which modeled by the spatial variables with plant axes MDS1, MDS2, and MDS3 as covariates (warm color corresponds to isoline –0.35, green color corresponds to isoline 0, and cold color corresponds to isoline 0.35); and (6) the values are presented which modeled by the spatial variables with plant axes MDS1, MDS2, MDS3, and MDS4 as covariates (warm color corresponds to isoline –0.35, green color corresponds to isoline 0, and cold color corresponds to isoline 0.35).

ecosystem (Kunakh et al., 2021). The intensity of tree influence varies horizontally and vertically. Trees change the properties of the soil in their close proximity (Binkley, Giardina, 1998). As the depth of soil layers increases, the influence of vegetation and soil biota decreases and the influence of weathering increases (Goebes et al., 2019). Soil properties adjacent to an individual tree vary with distance from the tree trunk according to radial symmetry (Zinke, 1962).

The medium-scale patterns of soil compaction variability are influenced by the herbaceous layer. The root system of herbaceous plants affects the physical condition of the soil. This influence mainly embraces the upper soil layer. Trees strongly influence the attributes of organic matter, which largely determines the distribution of forest understory plants (Oijen et al., 2005). The spatial organization of vegetation cover should be noted to be influenced by the physical and chemical variability of soil conditions. The variability of moisture content, soil acidity, and nutrient supply are important factors of such influence. While the influence of trees has a leveling effect, the influence of herbaceous plants leads to contrasting compaction in the soil profile. The decrease of compaction in the upper soil layer is accompanied by an increase of compaction in the middle soil layer. Soil compactness significantly affects plant root development. The root growth is reduced in compacted soils (Vocanson et al., 2006). A decrease in the rate of oxygen diffusion in compacted soils may be the cause of a decrease in the density of thin oak roots (Watson, Kelsey, 2006). The root growth rate and root elongation zone are reduced in compacted soils (Bengough, 1997; Lecompte et al., 2003). The plant roots become more tortuous with a greater density of branching and shorter lateral roots in compacted soils (Konôpka, 2009).

The variation in vegetation described by the NMDS4 measurement has no effect on soil penetration resistance. This influence can be assumed to have other frequency characteristics than those that can be accounted for in the present study. Obviously, to verify the hypothesis of their importance, the measurement of soil properties should be performed with a smaller sampling interval. The pure spatial component models the pedogenic variability of soil compaction. The processes of sediment deposition during floods affect the soil properties of floodplain soils and may be responsible for the formation of spatial patterns of soil compaction. The fluctuating groundwater level in the floodplain affects soil moisture supply and also regulates the ratio of oxidative and reducing conditions in the soil. These regimes are reflected in the packing level of soil particles in the soil, which entails variability in soil compaction.

Conclusion

The vegetation cover affects the horizontal and vertical patterns of variability in the soil penetration resistance of floodplain soils. The zone of a sharp increase in soil compaction with depth is associated with alluvial horizons. In the three-dimensional aspect, the components of variation of soil penetration resistance at different scales can be distinguished. The broad-scale component of variation is predominantly due to the influence of tree vegetation. The medium-scale component is due to the influence of herbaceous vegetation. The fine-scale component is independent of vegetation cover and influenced by pedogenic factors.

References

Assouline, S., Tessier, D. & Tavares-Filho J. (1997). Effect of compaction on soil physical and hydraulic properties: Experimental results and modeling. *Soil Sci. Soc. Am. J.*, 61(2), 390. DOI: 10.2136/sssaj1997.03615995006100020005x.

Benevenute, P.A.N., Morais, E.G., de Souza, A.A., Vasques, I.C.F., Cardoso, D.P., Sales, F.R., Severiano, E.C., Homem, B.G.C., Casagrande, D.R. & Silva B.M. (2020). Penetration resistance: An effective indicator for monitoring soil compaction in pastures. *Ecological Indicators*, 117, 106647. DOI: 10.1016/j.ecolind.2020.106647.

Bengough, A.G. (1997). Modelling rooting depth and soil strength in a drying soil profile. *J. Theor. Biol.*, 186(3), 327–338. DOI: 10.1006/jtbi.1996.0367

Bécel, C., Vercambre, G. & Pagès L. (2012). Soil penetration resistance, a suitable soil property to account for variations in root elongation and branching. *Plant Soil*, 353(1–2), 169–180. DOI: 10.1007/s11104-011-1020-7.

Binkley, D. & Giardina C. (1998). Why do tree species affect soils? The warp and woof of tree-soil interactions. *Biogeochemistry*, 42(1–2), 89–106. DOI: 10.1023/A:1005948126251.

Boivin, P., Schäffer, B., Temgoua, E., Gratier, M. & Steinman G. (2006). Assessment of soil compaction using soil shrinkage modelling: Experimental data and perspectives. *Soil Tillage Res.*, 88(1–2), 65–79. DOI: 10.1016/j.still.2005.04.008.

Borcard, D. & Legendre P. (2002). All-scale spatial analysis of ecological data by means of principal coordinates of neighbour matrices. *Ecol. Model.*, 153(1–2), 51–68. DOI: 10.1016/S0304-3800(01)00501-4.

Bray, J.R. & Curtis J.T. (1957). Anordination of the upland forest communities of Southern Wisconsin. *Ecol. Monogr.*, 27(4), 325–349. DOI: 10.2307/1942268.

Budakova, V.S., Yorkina, N.V., Telyuk, P.M., Umerova, A.K., Kunakh, O.M. & Zhukov O.V. (2021). Impact of recreational transformation of soil physical properties on micromolluscs in an urban park. *Biosystems Diversity*, 29(2), 78–87. DOI: 10.15421/012111.

Castrignanò, A., De Giorgio, D., Fornaro, F. & Vonella A.V. (2004). 3D spatial variation of soil impedance as affected by soil tillage. *ISCO 2004 – 13th International Soil Conservation Organisation Conference* (pp. 1–5). July 2004, Brisbane.

Colombi, T., Torres, L. C., Walter, A. & Keller T. (2018). Feedbacks between soil penetration resistance, root architecture and water uptake limit water accessibility and crop growth – A vicious circle. *Sci. Total Environ.*, 626, 1026–1035. DOI: 10.1016/j.scitotenv.2018.01.129.

Correa, J., Postma, J.A., Watt, M. & Wojciechowski T. (2019). Soil compaction and the architectural plasticity of root systems. *J. Exp. Bot.*, 70(21), 6019–6034. DOI: 10.1093/jxb/erz383.

De Neve, S. & Hofman G. (2000). Influence of soil compaction on carbon and nitrogen mineralization of soil organic matter and crop residues. *Biol. Fertil. Soils*, 30(5–6), 544–549. DOI: 10.1007/s003740050034.

Dexter, A.R., Czyż, E.A. & Gaţe O.P. (2007). A method for prediction of soil penetration resistance. *Soil Tillage Res.*, 93(2), 412–419. DOI: 10.1016/j.still.2006.05.011.

Ditzler, C.A., Engel, R.J. & Ahrens R.J. (2002). Soil taxonomy and soil survey. In H. Eswaran, T. Rice, R. Ahrens & B.A. Stewart (Eds.), *Soil classification* (pp. 1–10). CRC Press. DOI: 10.1201/9781420040364.

Dray, S., Bauman, D., Blanchet, G., Borcard, D., Clappe, S., Guenard, G., Jombart, T., Larocque, G., Legendre, P., Madi, N. & Wagner H.H. (2018). *Adespatial: Multivariate Multiscale Spatial Analysis. R package version 0.3-2. https://CRAN.R-project.org/package=adespatial.* https://rdrr.io/rforge/adespatial/

Dray, S., Pélissier, R., Couteron, P., Fortin, M.J., Legendre, P., Peres-Neto, P.R., Bellier, E., Bivand, R., Blanchet, F.G., De Cáceres, M., Dufour, A.B., Heegaard, E., Jombart, T., Munoz, F., Oksanen, J., Thioulouse, J. & Wagner H.H. (2012). Community ecology in the age of multivariate multiscale spatial analysis. *Ecol. Monogr.,* 82(3), 257–275. DOI: 10.1890/11-1183.1.

Fageria, N.K. & Stone L.F. (2006). Physical, chemical, and biological changes in the rhizosphere and nutrient availability. *J. Plant Nutr.*, 29(7), 1327–1356. DOI: 10.1080/01904160600767682.

Flinn, K.M. & Marks P.L. (2007). Agricultural legacies in forest environments: Tree communities, soil properties, and light availability. *Ecol. Appl.*, 17(2), 452–463. DOI: 10.1890/05-1963.

Gilbert, B. & Bennett J.R. (2010). Partitioning variation in ecological communities: Do the numbers add up? *J. Appl. Ecol.*, 47(5), 1071–1082. DOI: 10.1111/j.1365-2664.2010.01861.x.

Goebes, P., Schmidt, K., Seitz, S., Both, S., Bruelheide, H., Erfmeier, A., Scholten, T. & Kühn P. (2019). The strength of soil-plant interactions under forest is related to a Critical Soil Depth. *Scientific Reports*, 9(1), 8635. DOI: 10.1038/s41598-019-45156-5.

Holthusen, D., Brandt, A.A., Reichert, J.M. & Horn R. (2018). Soil porosity, permeability and static and dynamic strength parameters under native forest/grassland compared to no-tillage cropping. *Soil Tillage Res.*, 177, 113–124. DOI: 10.1016/j.still.2017.12.003.

Hout, M.C., Papesh, M.H. & Goldinger S.D. (2013). Multidimensional scaling. *Wiley Interdisciplinary Reviews: Cognitive Science*, 4(1), 93–103. DOI: 10.1002/wcs.1203.

Imhoff, S., Pires da Silva, A., Ghiberto, P.J., Tormena, C.A., Pilatti, M.A. & Libardi P.L. (2016). Physical quality indicators and mechanical behavior of agricultural soils of Argentina. *PLOS ONE*, 11(4), e0153827. DOI: 10.1371/journal.pone.0153827.

Jahn, R., Blume, H.P., Asio, V., Spaargaren, O. & Schad P. (2006). *Guidelines for soil description.* Rome: Food and Agriculture Organization of the United Nations.

Jones, C.G., Lawton, J.H. & Shachak M. (1994). Organisms as ecosystem engineers. *Oikos*, 69(3), 373. DOI: 10.2307/3545850.

Junior, D.D.V., Biachini, A., Valadão, F.C.A. & Rosa R.P. (2014). Penetration resistance according to penetration rate, cone base size and different soil conditions. *Bragantia*, *73*(2), 171–177. DOI: 10.1590/brag.2014.013.

Konôpka, B., Pagès, L. & Doussan C. (2009). Soil compaction modifies morphological characteristics of seminal maize roots. *Plant, Soil and Environment*, 55(1), 1–10. DOI: 10.17221/380-PSE.

Kovacic, I., Radomirovic, D., Zukovic, M., Pavel, B. & Nikolic M. (2018). Characterisation of tree vibrations based on the model of orthogonal oscillations. *Scientific Reports*, 8(1), 8558. DOI: 10.1038/s41598-018-26726-5.

Kozlowski, T.T. (1999). Soil compaction and growth of woody plants. *Scand. J. For. Res.*, 14(6), 596–619. DOI: 10.1080/02827589908540825.

Kruskal, J.B. (1964). Nonmetric multidimensional scaling: a numerical method. *Psychometrika*, 29, 115–129.

Krzic, M., Newman, R.F., Broersma, K. & Bomke A.A. (1999). Soil compaction of forest plantations in interior British Columbia. *J. Range Manag.*, 52(6), 671. DOI: 10.2307/4003640.

Kunakh, O.M., Lisovets, O.I., Yorkina, N.V. & Zhukova Y.O. (2021). Phytoindication assessment of the effect of reconstruction on the light regime of an urban park. *Biosystems Diversity*, 29(3), 84–93. DOI: 10.15421/012135.

Kunakh, O.N., Kramarenko, S.S., Zhukov, A.V., Zadorozhnaya, G.A. & Kramarenko A.S. (2018). Intra-population spatial structure of the land snail *Vallonia pulchella* (Müller, 1774) (Gastropoda; Pulmonata; Valloniidae). *Ruthenica*, 28(3), 91–99.

Kyle, G.P., Beard, K.H. & Kulmatiski A. (2007). Reduced soil compaction enhances establishment of non-native plant species. *Plant Ecol.*, 193(2), 223–232. DOI: 10.1007/s11258-006-9260-y.

Labelle, E.R., Poltorak, B.J. & Jaeger D. (2019). The role of brush mats in mitigating machine-induced soil disturbances: an assessment using absolute and relative soil bulk density and penetration resistance. *Can. J. For. Res.*, 49(2), 164–178. DOI: 10.1139/cjfr-2018-0324.

Lamandé, M., Hallaire, V., Curmi, P., Pérès, G. & Cluzeau D. (2003). Changes of pore morphology, infiltration and earthworm community in a loamy soil under different agricultural managements. *Catena*, 54(3), 637–649. DOI: 10.1016/S0341-8162(03)00114-0.

Lecompte, F., Ozier-Lafontaine, H. & Pages L. (2003). An analysis of growth rates and directions of growth of primary roots of field-grown banana trees in an andisol at three levels of soil compaction. *Agronomie*, 23(3), 209–218. DOI: 10.1051/agro:2002084.

Legendre, L. & Legendre P. (2012). *Numerical ecology*. Elsevier.

Lucas, M., Schlüter, S., Vogel, H.-J. & Vetterlein D. (2019). Roots compact the surrounding soil depending on the structures they encounter. *Scientific Reports*, 9(1), 16236. DOI: 10.1038/s41598-019-52665-w.

Medina, C., Camacho-Tamayo, J.H. & Cortés C.A. (2012). Soil penetration resistance analysis by multivariate and geostatistical methods. *Engenharia Agrícola*, 32(1), 91–101. DOI: 10.1590/S0100-69162012000100010.

Medvedev, V.V. (2009). Soil penetration resistance and penetrographs in studies of tillage technologies. *Eurasian Soil Science*, 42(3), 299–309. DOI: 10.1134/S1064229309030077.

Mohanty, M., Painuli, D. & Mandal K. (2004). Effect of puddling intensity on temporal variation in soil physical conditions and yield of rice (*Oryza sativa* L.) in a Vertisol of central India. *Soil Tillage Res.*, 76(2), 83–94. DOI: 10.1016/j.still.2003.08.006.

Mohanty, M. & Patra H.K. (2012). Effect of chelate-assisted Hhxavalent chromium on physiological changes, biochemical alterations, and chromium bioavailability in crop plants–an in vitro phytoremediation approach. *Bioremediat. J.*, 16(3), 147–155. DOI: 10.1080/10889868.2012.687414.

Mossadeghi-Björklund, M., Arvidsson, J., Keller, T., Koestel, J., Lamandé, M., Larsbo, M. & Jarvis N. (2016). Effects of subsoil compaction on hydraulic properties and preferential flow in a Swedish clay soil. *Soil Tillage Res.*, 156, 91–98. DOI: 10.1016/j.still.2015.09.013.

Mossadeghi-Björklund, M., Jarvis, N., Larsbo, M., Forkman, J. & Keller T. (2019). Effects of compaction on soil hydraulic properties, penetration resistance and water flow patterns at the soil profile scale. *Soil Use Manag.*, 35(3), 367–377. DOI: 10.1111/sum.12481.

Nawaz, M.F., Bourrié, G. & Trolard F. (2013). Soil compaction impact and modelling. A review. *Agronomy for Sustainable Development*, 33(2), 291–309. DOI: 10.1007/s13593-011-0071-8.

Netsvetov, M. & Nikulina V. (2010). Seasonal variations of oscillation and vibration parameters of *Acer platanoides*. *Dendrobiology*, 64, 37–42.

Nsabimana, G., Bao, Y., He, X., Nambajimana, J. de D., Wang, M., Yang, L., Li, J., Zhang, S. & Khurram D. (2020). Impacts of water level fluctuations on soil aggregate stability in the Three Gorges Reservoir, China. *Sustainability*, 12(21), 9107. DOI: 10.3390/su12219107.

Oijen, D., Feijen, M., Hommel, P., Ouden, J. & Waal R. (2005). Effects of tree species composition on within-forest distribution of understorey species. *Appl. Veg. Sci.*, 8(2), 155–166. DOI: 10.1111/j.1654-109X.2005.tb00641.x.

Oksanen, J., Blanchet, F. G., Friendly, M., Kindt, R., Legendre, P., McGlinn, D., Minchin, P.R., O'Hara, R.B., Simpson, G.L., Solymos, P., Stevens, M.H.H., Szoecs, E. & Wagner H. (2019). *vegan: Community Ecology Package. R package version 2.5-6. https://CRAN.R-project.org/package=vegan*. https://cran.r-project.org/package=vegan.

Plum, N. (2005). Terrestrial invertebrates in flooded grassland: A literature review. *Wetlands*, 25(3), 721–737. DOI: 10.1672/0277-5212(2005)025[0721:TIIFGA]2.0.CO;2.

Prokof'eva, T., Umarova, A., Bykova, G., Suslenkova, M., Ezhelev, Z., Kokoreva, A., Gasina, A. & Martynenko I. (2021). Morphological and physical properties in diagnostics of urban soils: case study from Moscow, Russia. *Soil Science Annual*, 71(4), 309–320. DOI: 10.37501/soilsa/131598.

Raunkiaer, C. (1937). *Plant life forms*. Oxford: Clarendon Press.

Roesch, A., Weisskopf, P., Oberholzer, H., Valsangiacomo, A. & Nemecek T. (2019). An approach for describing the effects of grazing on soil quality in life-cycle assessment. *Sustainability*, 11(18), 4870. DOI: 10.3390/su11184870.

Rozanov, B.G. (2004). *Soil morphology (in Russian)*. Moscow: Moscow University Press.

Schjønning, P., Lamandé, M., Munkholm, L.J., Lyngvig, H.S. & Nielsen J.A. (2016). Soil precompression stress, penetration resistance and crop yields in relation to differently-trafficked, temperate-region sandy loam soils. *Soil Tillage Res.*, 163, 298–308. DOI: 10.1016/j.still.2016.07.003.

Sinnett, D., Morgan, G., Williams, M. & Hutchings T.R. (2008). Soil penetration resistance and tree root development. *Soil Use Manag.*, 24(3), 273–280. DOI: 10.1111/j.1475-2743.2008.00164.x.

Tekin, Y., Kul, B. & Okursoy R. (2008). Sensing and 3D mapping of soil compaction. *Sensors*, 8(5), 3447–3459. DOI: 10.3390/s8053447.

Tracy, S.R., Black, C.R., Roberts, J.A. & Mooney S.J. (2011). Soil compaction: a review of past and present techniques for investigating effects on root growth. *J. Sci. Food Agric.*, 91(9), 1528–1537. DOI: 10.1002/jsfa.4424.

Unger, P.W. & Kaspar T.C. (1994). Soil compaction and root Growth: A review. *Agron. J.*, 86(5), 759–766. DOI: 10.2134/agronj1994.00021962008600050004x.

Vaz, C.M., Bassoi, L.H. & Hopmans J.W. (2001). Contribution of water content and bulk density to field soil penetration resistance as measured by a combined cone penetrometer–TDR probe. *Soil Tillage Res.*, 60(1–2), 35–42. DOI: 10.1016/S0167-1987(01)00173-8.

Vocanson, A., Roger-Estrade, J., Boizard, H. & Jeuffroy M.H. (2006). Effects of soil structure on pea (Pisum sativum L.) root development according to sowing date and cultivar. *Plant Soil*, 281(1–2), 121–135. DOI: 10.1007/s11104-005-3938-0.

Voronin, A.D. (1984). *Structural-functional hydrophysics of soils (in Russian)*. Moscow: Moscow State University Press.

Wang, X., Wang, C., Wang, X. & Huo Z. (2020). Response of soil compaction to the seasonal freezing-thawing process and the key controlling factors. *CATENA*, 184, 104247. DOI: 10.1016/j.catena.2019.104247.

Warton, D.I., Wright, S.T. & Wang Y. (2012). Distance-based multivariate analyses confound location and dispersion effects. *Methods in Ecology and Evolution*, 3(1), 89–101. DOI: 10.1111/j.2041-210X.2011.00127.x.

Watson, G.W. & Kelsey P. (2006). The impact of soil compaction on soil aeration and fine root density of Quercus palustris. *Urban Forestry and Urban Greening*, 4(2), 69–74. DOI: 10.1016/j.ufug.2005.08.001.

Westhoff, V. & Van Der Maarel E. (1978). The Braun-Blanquet Approach. In R.H. Whittaker (Ed.), *Classification of plant communities* (pp. 287–399). Dordrecht: Springer. DOI: 10.1007/978-94-009-9183-5_9.

WRB (2014). *World Reference Base for soil resources 2014: international soil classification system for naming soils and creating legends for soil maps*. World Soil Resources Reports No. 106. Rome: FAO.

Xu, J., Tang, Y. & Zhou J. (2017). Effect of drying–wetting cycles on aggregate breakdown for yellow–brown earths in karst areas. *Geoenvironmental Disasters*, 4(1), 20. DOI: 10.1186/s40677-017-0084-y.

Yakovenko, V. (2017). Fractal properties of coarse/fine-related distribution in forest soils on colluvium. In *Soil Science Working for a Living* (pp. 29–42). Cham: Springer International Publishing. DOI: 10.1007/978-3-319-45417-7_3.

Yakovenko, V. & Zhukov O. (2021). Zoogenic structure aggregation in steppe and forest soils. In Y. Dmytruk & D. Dent (Eds.), *Soils under stress* (pp. 111–127). Cham: Springer International Publishing. DOI: 10.1007/978-3-030-68394-8_12.

Yao, S., Teng, X. & Zhang B. (2015). Effects of rice straw incorporation and tillage depth on soil puddlability and mechanical properties during rice growth period. *Soil Tillage Res.*, 146, 125–132. DOI: 10.1016/j.still.2014.10.007.

Yorkina, N., Maslikova, K., Kunah, O. & Zhukov O. (2018). Analysis of the spatial organization of Vallonia pulchella (Muller, 1774) ecological niche in Technosols (Nikopol manganese ore basin, Ukraine). *Ecologica Montenegrina*, 17(1), 29–45.

Yorkina, N.V., Podorozhniy, S.M., Velcheva, L.G., Honcharenko, Y.V. & Zhukov O.V. (2020). Applying plant disturbance indicators to reveal the hemeroby of soil macrofauna species. *Biosystems Diversity*, 28(2), 181–194. DOI: 10.15421/012024.

Yudina, A.V., Fomin, D.S., Kotelnikova, A.D. & Milanovskii E.Y. (2018). From the notion of elementary soil particle to the particle-size and microaggregate-size distribution analyses: A review. *Eurasian Soil Science*, 51(11), 1326–1347. DOI: 10.1134/S1064229318110091.

Zadorozhnaya, G.A., Andrusevych, K.V. & Zhukov O.V. (2018). Soil heterogeneity after recultivation: Ecological aspect. *Folia Oecologica*, 45(1), 46–52. DOI: 10.2478/foecol-2018-0005.

Zelený, D. (2016). *Adjusted R2 in partial constrained ordination: the difference between R (vegan) and CANOCO 5*. David Zelený Blog. http://davidzeleny.net/blog/2016/09/08/adjusted-r2-in-partial-constrained-ordination-the-difference-between-r-vegan-and-canoco-5/

Zhang, Y., Zhang, Z., Ma, Z., Chen, J., Akbar, J., Zhang, S., Che, C., Zhang, M. & Cerdà A. (2018). A review of preferential water flow in soil science. *Can. J. Soil Sci.*, 98(4), 604–618. DOI: 10.1139/cjss-2018-0046.

Zhukov, A. & Gadorozhnaya G. (2016). Spatial heterogeneity of mechanical impedance of a typical chernozem: The ecological approach. *Ekológia (Bratislava)*, 35(3), 263–278. DOI: 10.1515/eko-2016-0021.

Zhukov, O., Kunah, O., Dubinina, Y., Zhukova, Y. & Ganzha D. (2019). The effect of soil on spatial variation of the herbaceous layer modulated by overstorey in an Eastern European poplar-willow forest. *Ekológia (Bratislava)*, 38(3), 253–272. DOI: 10.2478/eko-2019-0020.

Zhukov, O.V., Kunah, O.M. & Dubinina Y.Y. (2017). Sensitivity and resistance of communities: Evaluation on the example of the influence of edaphic, vegetation and spatial factors on soil macrofauna. *Biosystems Diversity*, 25(4), 328–341. DOI: 10.15421/011750.

Zhukov, O.V., Kunah, O.M., Dubinina, Y.Y., Fedushko, M.P., Kotsun, V.I., Zhukova, Y.O. & Potapenko O.V. (2019). Tree canopy affects soil macrofauna spatial patterns on broad- And meso-scale levels in an Eastern European poplar-willow forest in the floodplain of the River Dnipro. *Folia Oecologica*, 46(2), 101–114. DOI: 10.2478/foecol-2019-0013.

Zhukov, O.V., Kunah, O.M., Dubinina, Y.Y. & Novikova V.O. (2018). The role of edaphic, vegetational and spatial factors in structuring soil animal communities in a floodplain forest of the Dnipro river. *Folia Oecologica*, 45(1), 8–23. DOI: 10.2478/foecol-2018-0002.

Zhukova, Y.O., Yorkina, N.V., Budakova, V.S. & Kunakh O.M. (2020). The small-scale variation of herb-layer community structure in a riparian mixed forest. *Biosystems Diversity*, 28(4), 390–398. DOI: 10.15421/012050.

Zinke, P.J. (1962). The pattern of influence of individual forest trees on soil properties. *Ecology*, 43(1), 130–133. DOI: 10.2307/1932049.